Efficient network flooding and time synchronization with Glossy

Conference Paper · May 2011

Source: IEEE Xplore

Federico Ferrari
ETH Zurich

Marco Zimmerling
Technische Universität Dresden

Olga Saukh
Graz University of Technology

Efficient Network Flooding and Time Synchronization with Glossy

Federico Ferrari Marco Zimmerling Lothar Thiele Olga Saukh
Computer Engineering and Networks Laboratory
ETH Zurich, Switzerland
{ferrari, zimmerling, thiele, saukh}@tik.ee.ethz.ch

ABSTRACT

This paper presents Glossy, a novel flooding architecture for wireless sensor networks. Glossy exploits constructive interference of IEEE 802.15.4 symbols for fast network flooding and implicit time synchronization. We derive a timing requirement to make concurrent transmissions of the same packet interfere constructively, allowing a receiver to decode the packet even in the absence of capture effects. To satisfy this requirement, our design temporally decouples flooding from other network activities. We analyze Glossy using a mixture of statistical and worst-case models, and evaluate it through experiments under controlled settings and on three wireless sensor testbeds. Our results show that Glossy floods packets within a few milliseconds and achieves an average time synchronization error below one microsecond. In most cases, a node receives the flooding packet with a probability higher than 99.99 %, while having its radio turned on for only a few milliseconds during a flood. Moreover, unlike existing flooding schemes, Glossy's performance exhibits no noticeable dependency on node density, which facilitates its application in diverse real-world settings.

Categories and Subject Descriptors

C.2.1 [**Computer-Communication Networks**]: Network Architecture and Design—*wireless communication*; C.2.2 [**Computer-Communication Networks**]: Network Protocols

General Terms

Design, Experimentation, Performance

Keywords

Network Flooding, Time Synchronization, Concurrent Transmissions, Constructive Interference, Wireless Sensor Networks

1. INTRODUCTION

Network flooding and time synchronization are two fundamental services in wireless sensor networks; they form the basis for a wide range of applications and network operations.

Many real-world applications rely on a seamless coexistence of both services. For instance, high-rate data collection systems synchronize nodes to correlate measurements, and use flooding to adjust sampling rates and trigger data downloads [33]. Most of these applications run two protocols in parallel (*e.g.*, Trickle [19] and FTSP [22]), which complicates their design and may cause protocol interactions that impair system performance [5]. A flooding service that implicitly synchronizes all nodes in the network could effectively avoid these problems.

Such an integrated service should flood packets as fast as possible to reduce inaccuracies introduced by clock drift [18]. Moreover, rapid flooding can enhance the performance of several applications [21]. In surveillance systems, for example, a node detecting an event needs to quickly wake up all other nodes to initiate group formation and collaborative signal processing [20].

Challenges. Rapid flooding is difficult in wireless networks where packet loss is a common phenomenon [37]. Retransmissions to recover lost packets help to overcome this problem. However, simple broadcasting results in serious medium contention, known as the broadcast storm problem [23]. To reduce the transmission overhead, nodes need to acknowledge broadcasts using sophisticated modulation schemes [8], encode redundancy into packets prior to transmission [24], or collect substantial information from neighboring nodes to decide whether a retransmission is necessary [35]. Therefore, loss recovery generally sacrifices latency and energy for an increased reliability.

Alternatively, reliability can be improved by reducing the risk of packet loss in the first place. One possible approach is to schedule broadcasts so that they do not interfere with each other. However, determining an interference-free broadcast schedule is an NP-complete problem [12] and subject to sudden topology changes.

In fact, due to the capture effect, a node can receive a packet despite interference from other wireless transmitters [17]. While the capture effect helps to improve flooding efficiency, it suffers from scalability problems in areas of high node density: the probability of receiving a packet decreases considerably as the number of overlapping transmissions increases [21].

Contribution and road-map. To tackle the issues above, we propose Glossy, a new flooding architecture for wireless sensor networks. Glossy considers interference an advantage rather than a problem. Unlike previous work, it makes *simultaneous transmissions of the same packet interfere constructively*, allowing receivers to decode the packet even in the absence of capture effects. In this way, Glossy achieves a flooding reliability above 99.99 % and approaches the theoretical lower latency bound across diverse node densities and network sizes. Moreover, Glossy provides network-wide time synchronization for free, since it implicitly synchronizes nodes as the flooding packet propagates through the network.

IPSN'11, April 12–14, 2011, Chicago, Illinois.

This paper makes the following contributions:

- We study in Sec. 2 why and under which conditions overlapping transmissions of the same packet interfere constructively. Our analysis reveals a strong dependency on the modulation scheme. Based on this insight, we show that the temporal offset among concurrent IEEE 802.15.4 transmitters must not exceed 0.5 μs to generate constructive interference with high probability.
- We introduce Glossy, a new flooding architecture for wireless sensor networks. Glossy exploits concurrent transmissions, time-synchronizes nodes, and decouples flooding from other network activities. We give an overview of Glossy's design in Sec. 3, and detail its radio-driven execution model in Sec. 4.
- We demonstrate in Sec. 5 the feasibility of Glossy with an implementation in Contiki [1] based on Tmote Sky sensor nodes. We describe how our implementation reduces time uncertainties on the nodes during packet relaying, and give guidelines for porting Glossy to other popular hardware platforms.
- We present in Sec. 6 a mixture of stochastic and worst-case models to analyze the robustness of our techniques in generating constructive interference. Applying these models to our implementation, we find that Glossy satisfies the 0.5 μs requirement with a probability higher than 99.9 % for 30 concurrent transmitters.

In Sec. 7, we evaluate Glossy using experiments under controlled settings and on three wireless sensor testbeds, including Twist [14] and MoteLab [34]. For example, we find that Glossy achieves an average time synchronization error below 0.4 μs, even at nodes that are eight hops away from the initiator of a flood. On Twist, at the lowest transmit power that keeps the network fully connected, we observe that nodes receive an 8-byte flooding packet within 3 ms; nodes receive the packet with a probability above 99.99 %, and have their radios turned on for less than 10 ms during a flood.

In light of our contributions, we survey related work in Sec. 8, and end the paper in Sec. 9 with brief concluding remarks.

2. CONCURRENT TRANSMISSIONS

Glossy exploits concurrent transmissions for efficient flooding in sensor networks. In this section, we investigate the conditions for making concurrent transmissions of the same packet interfere in a constructive way, so that a receiver detects the packet with high probability. We give some background on wireless interference and the IEEE 802.15.4 modulation scheme, based on which we determine a timing requirement for generating constructive interference.

2.1 Background

The broadcast nature of wireless communications causes interference whenever spatially close stations transmit concurrently; that is, when they generate signals that overlap in time and space, and share the same frequency. Interference generally reduces the probability that a receiver correctly detects the information embedded into the signals, even when the signals carry the same information. In the following discussion we focus on *baseband* signals, that is, sequences of IEEE 802.15.4 symbols. As we show in Sec. 7, the superposition of several, possibly out-of-phase *carrier* signals allows for correct detection with high probability, especially when more than three nodes transmit concurrently.

Constructive and destructive interference. Interference is *constructive* if a receiver detects the superposition of the baseband signals generated by multiple transmitters. By contrast, interference is *destructive* if it prevents a receiver from correctly detecting the superimposed baseband signals. In sensor networks, constructive interference has not been extensively exploited, due to the difficulty of achieving sufficiently accurate synchronization and the requirement of highly predictable software delays [30]. Several protocols [21] exploit instead the *capture effect*, which occurs when a wireless radio detects a signal from one transmitter despite the interference from other transmitters. A radio may capture one signal when it is stronger than the others (*power capture* [17]), or when it starts being received significantly earlier than the others (*delay capture* [7]). However, the capture effect suffers from scalability problems when many transmissions overlap, leading to packet loss [21].

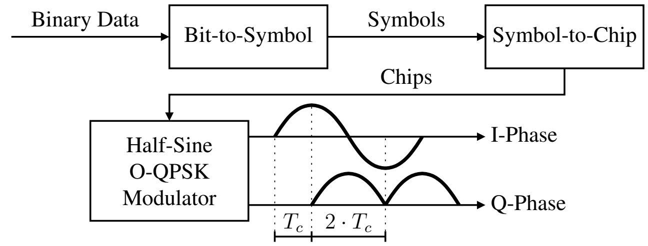

Figure 1: IEEE 802.15.4 modulation. *Using a three-step process, binary data are converted into a modulated signal.*

Requirements for generating constructive interference strongly depend on the communication scheme, especially on the modulation and the bit rate. We first review the specifications of the IEEE 802.15.4 standard. Then, we derive an *upper bound on the temporal displacement* Δ among multiple concurrent transmissions of the same packet that allows to correctly receive the packet with high probability due to constructive interference.

IEEE 802.15.4 modulation. The IEEE 802.15.4 standard [15] for wireless devices operating in the 2,450 MHz band employs an offset quadrature phase-shift keying (O-QPSK) modulation scheme with half-sine pulse shaping, which is equivalent to minimum-shift keying (MSK). Binary data are converted into a modulated analog signal using a three-step conversion process, as shown in Fig. 1.

First, data are grouped into 4-bit *symbols*. Each symbol is then mapped to a *pseudo-random noise (PN) sequence* of 32 bits, where each bit of such a sequence is called *chip*. PN sequences add redundancy, and relate to each other through cyclic shifts and conjugation of chips. In a last step, each PN sequence is modulated onto the carrier signal using O-QPSK with half-sine pulse shaping. That is, even-indexed chips are modulated onto the *in-phase (I)* carrier, odd-indexed chips onto the *quadrature-phase (Q)* carrier. Q-phase chips are delayed by $T_c = 0.5\,\mu$s with respect to I-phase chips to get a $\pi/2$ phase change. Overall, a new chip is transmitted every T_c, leading to a transmission rate of 250 kbps.

Demodulation at a receiver follows the opposite flow: each half-sine pulse is converted into a chip, and the resulting PN sequence into a symbol. Radios make only soft decisions for each chip [31]: the received PN sequence may contain non-binary values between 0 and 1. Hard decisions are made by selecting out of the 16 PN sequences the one that has the highest correlation with respect to the received PN sequence. In this step, the redundancy contained in a PN sequence increases the chances of a correct symbol detection, even if some chips are not correctly received.

Next, we show how the IEEE 802.15.4 standard translates into a maximum temporal displacement $\Delta_{\max}$ among multiple transmissions to generate constructive interference with high probability.

2.2 Generating Constructive Interference

Several studies [6, 36] estimate the bit error rate (BER) when receiving delayed replica of the same MSK signal. They show that the BER increases exponentially with the temporal displacement Δ among overlapping signals. However, as explained above, sensor network radios make hard decisions at the symbol level (*i.e.*, on PN sequences of 32 consecutive chips). The redundancy included in

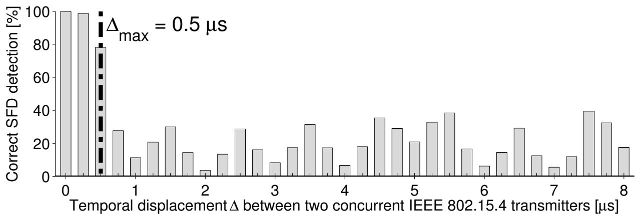

Figure 2: IEEE 802.15.4 transmitters interfere constructively if the temporal displacement is smaller than $\Delta_{\max} = 0.5\mu$s.

each PN sequence helps to tolerate decoding errors of single chips. Therefore, computing the error on a sequence of symbols provides a better estimation of the reception behavior of a sensor node.

We perform Matlab simulations to evaluate the maximum temporal displacement between two IEEE 802.15.4-compliant signals such that they interfere constructively with high probability. A receiver decodes the superposition of two signals. Each signal is generated by converting the start of frame delimiter (SFD) symbols specified by the IEEE 802.15.4 standard, first into a PN sequence and then into an MSK-modulated baseband signal. Both signals have the same amplitude, but one of them is delayed by a variable displacement with 250 ns granularity in the interval $[0, 8]$ μs. White Gaussian noise is added to the superimposed signal, resulting in a signal-to-noise ratio of -10 dB.

The receiver demodulates the superimposed signal. It then correlates each PN sequence with all 16 possible PN sequences and chooses the one with the highest correlation. This procedure resembles the operations of a IEEE 802.15.4 radio during a packet reception. Only if both SFD symbols are correctly estimated, the superimposed signal is considered correctly detected.

Fig. 2 shows the fraction of correctly detected signals depending on the temporal displacement Δ, averaged over 1,000 experiments with different seeds for the random noise. The signal is always correctly detected when $\Delta = 0$. Even for $\Delta = 0.25\,\mu$s the signal is correctly detected in more than 98 % of the cases. However, the fraction of correct detections starts to decrease significantly for a displacement larger than 0.5 μs, which corresponds to the chip period T_c. Interestingly, for increasing Δ, the fraction experiences local minima when Δ is a multiple of $2 \cdot T_c$, that is, when different chips perfectly overlap. Between two local minima, the redundancy added by the PN sequences increases the chances for a correct signal detection, despite errors on single chips. We verify using various symbol sequences and noise seeds that these results are independent of the specific symbol sequence of the SFD.

These simulations show that the probability of a correct detection is very high when identical IEEE 802.15.4 signals are generated with a time displacement below $\Delta_{\max} = 0.5\,\mu$s. A correct detection is entirely due to the modulation scheme and the redundancy encoded in PN sequences. On real nodes, capture effects can further increase the chances to correctly detect a packet, especially with high temporal or strength differences between the signals. We show in the following how the design and the implementation of Glossy strive to satisfy the requirement of $\Delta_{\max} = 0.5\,\mu$s, allowing nodes to receive packets even in the absence of beneficial capture effects (*e.g.*, when many nodes transmit concurrently).

3. GLOSSY OVERVIEW

We introduce Glossy, a new flooding architecture for wireless sensor networks. Glossy incorporates three main techniques.

Concurrent transmissions. Wireless is a broadcast medium, creating the opportunity for nodes to overhear packets from neighboring nodes. Using Glossy, nodes turn on their radios, listen for communications over the wireless medium, and relay overheard packets immediately after receiving them. Since the neighbors of a sender receive a packet at the same time, they also start to relay the packet at the same time. This again triggers other nodes to receive and relay the packet. In this way, Glossy benefits from concurrent transmissions by quickly propagating a packet from a source node (*initiator*) to all other nodes (*receivers*) in the network.

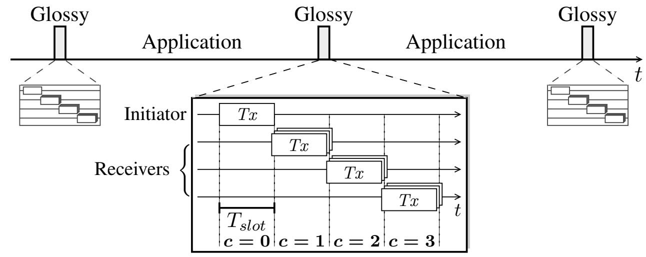

Figure 3: Glossy decouples flooding from other application tasks executing on the nodes. *The slot length T_{slot} is the time between transmissions of packets with relay counter c and c + 1. Nodes transmit packets with the same relay counter concurrently.*

An important property of Glossy is that, besides the first transmission of the initiator, *the flooding process is entirely driven by radio events*. For instance, a node triggers a transmission only when the radio signals the completion of a packet reception. As explained in Sec. 2, concurrent transmissions must be properly aligned to enable a receiver to successfully decode the packet. Glossy's radio-driven execution is a key factor to meet this requirement.

Time synchronization. Glossy exploits the above flooding mechanism to implicitly time-synchronize the nodes. It embeds into each packet a 1-byte field, the *relay counter c*. The initiator sets $c = 0$ before the first transmission. Nodes increment c by 1 before relaying a packet. Consequently, a node can infer from the relay counter how many times a received packet has been relayed.

As indicated in the lower part of Fig. 3, we define the time between the start of a packet transmission with relay counter c and the start of the following packet transmission with relay counter $c{+}1$ as the *slot length* T_{slot}. Nodes locally estimate T_{slot} using timestamps taken at the occurrence of radio interrupts. Most importantly, T_{slot} is a network-wide constant, since during a flood nodes never alter the packet length. Based on the relay counter c of a received packet and the estimate of T_{slot}, a node computes the time at which the initiator started the flood, called the *reference time*. In this way, all receivers synchronize relatively to the clock of the initiator. To achieve absolute time synchronization, the initiator embeds its own clock value into the flooding packet.

Temporal decoupling. A time-synchronized network is useful for many purposes. Glossy benefits from it by temporally decoupling network flooding from *all* other application tasks executing on the nodes, as depicted in the upper part of Fig. 3. In particular, nodes know the interval between two Glossy phases (*e.g.*, by embedding the interval into packets injected by the initiator), which allows them to synchronously stall other tasks right before a flood and to resume these tasks immediately afterwards. As a result, Glossy never interferes with other activities, leading to a highly deterministic behavior during a flood. Temporal decoupling is thus another key factor to make concurrent transmissions precisely overlap.

Moreover, temporal decoupling allows the network to run other protocols or execute other tasks between two network floods. For example, an application may use a data collection protocol on top of a low-power MAC to gather sensory data, while at regular intervals Glossy takes over to disseminate commands to the nodes (*e.g.*, to

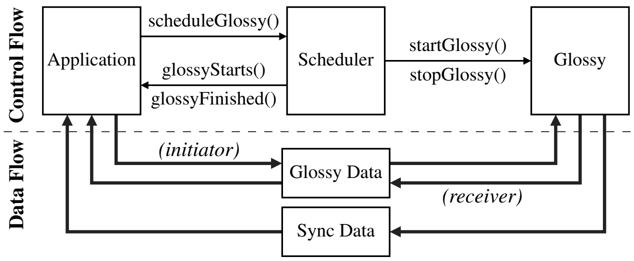

Figure 4: Example of Glossy as an application service. *An application instructs a scheduler to run Glossy periodically. The scheduler notifies the application about an upcoming Glossy phase.*

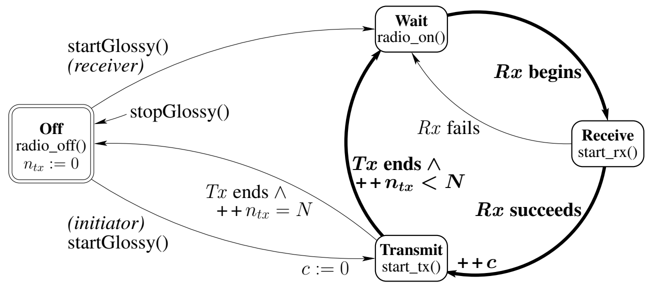

Figure 5: States of Glossy during execution. *Transitions in the main state sequence (bold arrows) are triggered by radio events.*

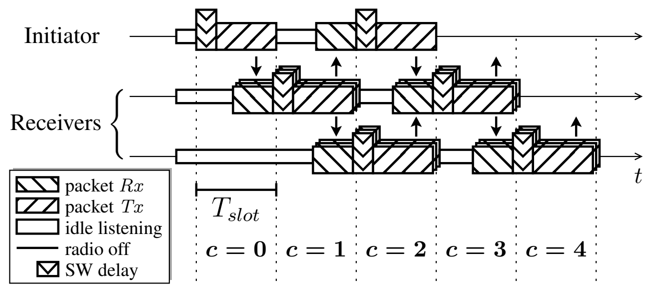

Figure 6: Example of a Glossy flood with $N = 2$. *Nodes always transmit packets with the same relay counter c concurrently.*

adjust the sampling rate) and to keep the nodes synchronized. Here, also the application benefits from temporal decoupling, since flooding packets never interfere with data collection packets. Such protocol interference could substantially degrade system performance, especially in terms of data yield [5].

Glossy integrates smoothly with a software system that provides primitives to decouple tasks over time, such as the slotted programming approach [13]. Duty-cycled networks, where all nodes wake up at the same time [4], can allocate Glossy at the beginning of the active phase, or during the sleep phase when no other communication takes place. Nevertheless, as demonstrated by our experiments in Sec. 7, Glossy needs only a few milliseconds to complete.

Fig. 4 shows a possible way of integrating Glossy with the rest of the software system on a node. An *application* that wishes to use it instructs the *scheduler* using scheduleGlossy() to run Glossy with a certain period. This period can be changed by the application at runtime (*e.g.*, upon receiving a new interval from the initiator) by calling the same function again. Depending on the period, the scheduler starts and stops Glossy, using functions startGlossy() and stopGlossy() provided by the Glossy interface. Moreover, the scheduler notifies the application in advance via callback function glossyStarts() before it starts Glossy, giving the application the opportunity to prepare for Glossy taking over. Similarly, the scheduler notifies the application via callback function glossyFinished() after Glossy has terminated.

This *control flow* is the same for both initiator and receiver, but the *data flow* is not, as shown in the lower part of Fig. 4. On the initiator, the application provides Glossy with the data to be flooded. On the receiver, Glossy passes the received data to the application. Glossy provides the synchronization data (*i.e.*, the reference time) to the applications of both, initiator and receiver.

At system startup, when a receiver is not yet synchronized, the application may instruct the scheduler to run Glossy with a shorter period in order to quickly overhear a Glossy packet from other nodes and get synchronized. By adapting the period, sophisticated mechanisms [9] can be implemented to achieve the desired trade-off between fast initial synchronization and energy efficiency.

Glossy manages interrupts and timers transparently. It masks software and hardware interrupts that are not essential to its functioning and disables all hardware timers. Nevertheless, Glossy records which interrupts have been active and which timers have been scheduled before its execution. Using this information, Glossy restores interrupts and timers after it terminates, allowing the application and the rest of the system to smoothly continue its execution.

4. GLOSSY IN DETAIL

This section describes the Glossy architecture in detail. We first illustrate the sequence of operations executed during a flood, followed by an analysis of the timing behavior of these operations.

4.1 Radio-driven Execution Model

Fig. 5 depicts the core of Glossy, represented by the repetitive sequence of states **Wait** → **Receive** → **Transmit**. The scheduler starts Glossy using startGlossy(). Afterwards, a receiver begins the execution in the **Wait** state. The initiator, instead, starts from state **Transmit**, and transmits a packet with relay counter $c = 0$. After this startup phase, the execution is the same for both initiator and receivers, as described in the following.

In the **Wait** state, a node has its radio turned on and waits for a packet being flooded through the network. When the radio indicates the beginning of a reception, the microcontroller unit (MCU) starts to read the incoming packet. This action corresponds to a transition to the **Receive** state. If the reception fails (*e.g.*, due to packet corruption), the node returns to the **Wait** state. Otherwise, if the reception succeeds, the node makes a transition to the **Transmit** state. In this case, the MCU immediately issues a transmission request to the radio, increments the relay counter c by 1, and copies the modified packet from the receive (Rx) buffer to the transmit (Tx) buffer. To introduce only a small and predictable delay, the MCU performs this packet copying *after* issuing the transmission request, that is, while the radio switches from Rx to Tx mode. In Sec. 5, we demonstrate the feasibility of this approach on common sensor node platforms. Some recent radios feature a single packet buffer [3], making the packet copying step obsolete.

Nodes can transmit a packet multiple times to increase flooding reliability. We denote with N the *maximum number of times a node transmits during a flood*. When a packet transmission ends, a *transmission counter* n_{tx} is incremented and compared to the maximum number of transmissions N. If a node has already transmitted N times, it makes a transition to state **Off**, turns off the radio, and Glossy completes. Otherwise, the node returns to the **Wait** state, and the sequence starts again at the next packet reception. Ultimately, the scheduler stops Glossy by calling stopGlossy().

Fig. 6 shows an example of a network flood with $N = 2$. When Glossy starts, the initiator sets the relay counter c to 0 and transmits the first time to start the flooding process. Receivers within com-

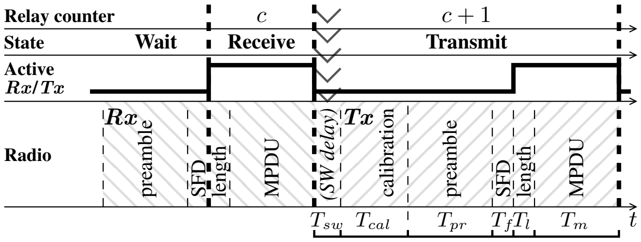

Figure 7: Timeline of main Glossy states. *The radio determines the dwell time of each state, except for the time required to trigger a packet transmission, T_{sw}, which is determined by the MCU.*

munication range of the initiator overhear the packet, set c to 1, and transmit concurrently. Their neighboring nodes, *including the initiator*, overhear this second packet, set c to 2, and again transmit concurrently. In this way, nodes always transmit packets with the same relay counter c concurrently. The process repeats until n_{tx} reaches N at all nodes in the network. In Sec. 7, we further investigate the impact of N on the performance of Glossy.

All transitions among states in Glossy's main loop in Fig. 5 are triggered by radio events. On standard sensor network platforms, the MCU is typically notified of these events through interrupts. Therefore, the few software operations required by Glossy are executed within interrupt service routines (ISRs). In Sec. 5, we describe an implementation of Glossy that limits uncertainties in the execution time to inaccuracies of the underlying hardware.

4.2 Execution Timing

The dwell time of the main Glossy states depends primarily on the radio hardware. The MCU influences the timing only after the completion of a packet reception, and only for the time necessary to trigger a packet transmission.

Fig. 7 shows the timeline of the main Glossy state sequence. We see that the timing depends only on the radio, besides a short period at the beginning of the **Transmit** state. We call this period the *software delay* T_{sw}, required by the MCU to trigger a packet transmission. This delay depends primarily on the software routine. In addition, it is affected by the frequency of the serial peripheral interface (SPI) bus that is used on most sensor node platforms for the communication between the MCU and the radio.

In Sec. 3, we discussed that a receiver computes the synchronization reference time based on the estimate of the slot length T_{slot}, defined as the time between the start of two packet transmissions with relay counter c and $c+1$. We now show that T_{slot} mostly depends on the radio hardware, which is an important property to achieve high synchronization accuracy. We analyze in Sec. 6 how hardware inaccuracies influence the slot length. T_{slot} accounts for the software delay T_{sw}, the time required to transmit a packet T_{tx}, and the processing delay T_d introduced by the radio at the beginning of a packet reception. T_{slot} can thus be expressed as:

$$T_{slot} = T_{sw} + T_{tx} + T_d \tag{1}$$

We provide an analytical expression for the time required to transmit a packet T_{tx}. Fig. 7 shows the operations performed by the radio during a packet transmission. Once the radio receives a transmission request, it starts to calibrate the internal voltage controlled oscillator (VCO). We denote the hardware-dependent time required for this calibration with T_{cal}. A valid IEEE 802.15.4 packet consists of the following fields: (*i*) the preamble composed of 8 `0x0` symbols, (*ii*) the SFD corresponding to symbols `0x7A`, (*iii*) the 2-symbol frame length field that specifies the number of bytes L_m contained in the MAC protocol data unit (MPDU), and (*iv*) the MPDU itself that carries the application data. We denote with T_{pr}, T_f, T_l, and T_m the times required to transmit each of these fields. The time needed for a packet transmission is thus given by:

$$T_{tx} = T_{cal} + T_{pr} + T_f + T_l + T_m \tag{2}$$

Note that in (2) only T_m depends on the packet length. The other terms are determined by the radio hardware and the standard.

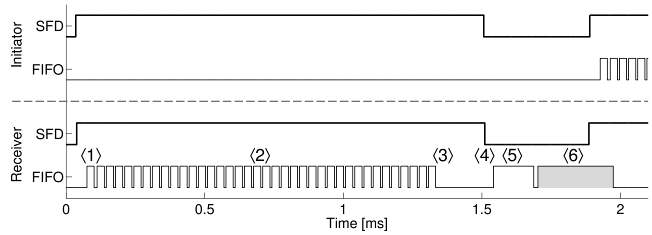

Figure 8: Data transfer between the radio buffers and the MCU in Glossy. *Snapshot taken with a logic analyzer during the transmission of a 46-byte packet. Data transfers (FIFO pin) from the radio's Rx buffer are denoted in white, to the Tx buffer in gray.*

5. IMPLEMENTATION

We implemented Glossy in Contiki [1] based on Tmote Sky sensor nodes, which feature an MSP430 microcontroller [32] and a CC2420 radio [31] compliant with the IEEE 802.15.4 standard. In this section we first show how our implementation leads to a highly deterministic software delay, which is a necessary condition to generate constructive interference (see Sec. 2). We then outline the approach we use to achieve high synchronization accuracy. Finally, we provide guidelines for porting Glossy to different radios.

Software instructions are executed by the MCU, whose clock is sourced by a digitally controlled oscillator (DCO). The DCO frequency varies with temperature, voltage, and from device to device. Although digital control allows to stabilize the frequency on a long-term basis (*e.g.*, using the more stable external 32,768 Hz crystal as a reference), short-term stability is not guaranteed. The frequency of the DCO can deviate up to $\pm 20\,\%$ from the nominal value, with temperature and voltage drifts of -0.38 %/°C and 5 %/V [32]. To counteract these variations, our Glossy implementation (*i*) strives to *minimize* the number of software instructions, mitigating the impact of DCO instability on the software delay, and (*ii*) ensures a *constant* number of software instructions. Moreover, the DCO runs independently of the radio clock, leading to varying delays in the transfer of digital signals between the radio circuit and the MCU. Therefore, our implementation (*iii*) compensates for varying offsets between the DCO and the radio clock. In the following, we describe these aspects of our implementation.

5.1 Minimizing Software Delay

We exploit buffered packet receptions and transmissions to minimize the number of software instructions. The CC2420 radio provides two buffers for receiving (Rx) and transmitting (Tx), implemented as first-in-first-out queues. During a packet reception, the radio stores incoming data into the Rx buffer. The FIFO pin signals the MCU when the Rx buffer contains at least 1 byte. The MCU never enters a low-power mode while Glossy is running, so that all of its components are always enabled.

Glossy can flood packets of any IEEE 802.15.4-compliant length. During a reception, a receiver checks the length of the packet being flooded by reading the first byte of the packet, corresponding to the packet length field. This action corresponds to step ⟨1⟩ in Fig. 8, which shows the sequence of data transfers between the radio buffers and the MCU measured with a logic analyzer. If the packet length is greater than 8 bytes, Glossy lets the MCU poll the FIFO pin: the content of the packet is read byte after byte over the SPI bus and stored into a temporary buffer while the packet is still being received by the radio $\langle 2 \rangle$. When only 8 bytes are left to receive, Glossy stops polling the FIFO pin $\langle 3 \rangle$, and waits until the SFD pin makes a transition to 0 and an interrupt occurs. At this point, Glossy executes a minimum, constant number of software instructions just to serve the interrupt and to issue a transmission request to the radio $\langle 4 \rangle$. Then, while the radio calibrates the VCO, Glossy reads the last 8 bytes $\langle 5 \rangle$ from the Rx buffer, and checks whether the packet has been received successfully. If so, Glossy increments the relay counter c and copies the data from the temporary buffer into the Tx buffer of the radio $\langle 6 \rangle$, which then transmits the packet; otherwise, Glossy aborts the transmission process before the radio actually starts sending the preamble. When the packet length is at most 8 bytes, Glossy skips polling the FIFO pin (steps $\langle 2 \rangle$ and $\langle 3 \rangle$), and reads the remaining content of the Rx buffer after the packet reception completes.

This approach is feasible as it takes only a few software instructions to check whether a packet has been successfully received; the MCU executes these instructions and starts writing to the Tx buffer before the radio completes the VCO calibration. For long packets, the Tx buffer might not be completely filled before the radio starts transmitting the first bytes from the Tx buffer, as is the case in Fig. 8. This does not cause a buffer underflow, since the Tx buffer is a first-in-first-out queue and copying data over the SPI bus is faster than transmitting it over the wireless medium. In our implementation, the latency required for writing to the Tx buffer is 5.75 μs per byte, plus an initial latency of 18 μs; the time required to transmit a byte with an IEEE 802.15.4-compliant radio is 32 μs.

5.2 Making Software Delay Deterministic

A small and constant number of software instructions does not guarantee that the MCU issues a transmission request to the radio a constant number of cycles after being notified of the end of a packet reception. When the MCU receives an interrupt request, it first completes the execution of the current instruction before starting to serve the interrupt. Instructions on the MSP430 require between 1 and 6 clock cycles to complete. Interrupts are thus served with a variable delay, depending on which instruction is being executed when the MCU receives the interrupt.

Glossy compensates for this variable delay by measuring the number of clock ticks elapsed between the instant at which the interrupt is received, recorded using the capture functionality of the MCU at the rising edge of the SFD pin, and the instant at which it is served. Depending on the measured delay, Glossy inserts a certain number of *no operations (NOPs)* at the beginning of the interrupt handler. Glossy thus ensures that a transmission request to the radio is issued a constant number of clock cycles after the interrupt reception, which makes the software delay highly deterministic.

5.3 Compensating for Hardware Variations

The software delay T_{sw} is the sum of (*i*) the time required by the MCU to sample the transition of the radio's SFD pin at the end of a packet reception, (*ii*) the number of MCU clock ticks I needed to issue a transmission request to the radio, and (*iii*) the time required by the radio to sample the transmission request coming from the MCU. Using the mechanisms described above, we know that I is constant in our implementation. However, due to the asynchronous clocks of radio and MCU, the software delay T_{sw} is still not constant: there is a variable delay in the transfer of digital signals between these two components.

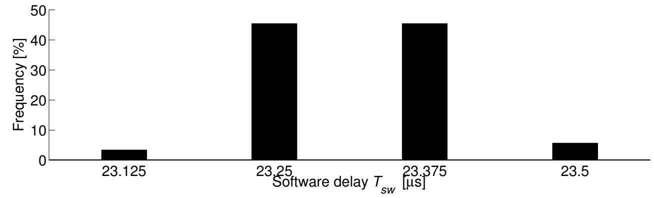

Figure 9: Distribution of the software delay T_{sw}. *Results from a logic analyzer show that in 91 % of the cases T_{sw} matches the theoretical binary distribution of two values with a distance of one radio clock tick, corresponding to 125 ns.*

The radio updates its digital output signals with frequency f_r, determined by its crystal oscillator. The internal DCO determines the frequency f_p of the MCU. Neglecting clock drifts, we can write:

$$T_{sw} = \frac{1}{f_r} \cdot \left\lceil (I + k_p) \cdot \frac{f_r}{f_p} \right\rceil \tag{3}$$

where k_p ($0 < k_p \leq 1$) is the fraction of the DCO period $1/f_p$ required at the MCU to sample the SFD transition at the end of the packet reception. Given that the radio clock and the DCO run completely unsynchronized, the initial offset k_p is a continuous random variable uniformly distributed in the interval $0 < k_p \leq 1$. This implies that T_{sw} is a discrete random variable with granularity $1/f_r$. The number of possible discrete values for T_{sw} and their distribution depend on the number of DCO ticks I.

By inserting a constant number of NOPs, we choose I in our implementation so that we obtain from (3) a distribution that achieves the theoretical lower bound of only two possible values for T_{sw}. These two values are $1/f_r$ apart—as long as radio and MCU use two independent clocks, any implementation of Glossy exhibits a minimum jitter of $1/f_r$ in the software delay. For example, on the Tmote Sky, the CC2420 radio updates its digital output signals with frequency $f_r = 8$ MHz, and the DCO of the MSP430 runs in our implementation at a frequency $f_p = 4,194,304$ Hz. The resulting difference between the two possible values of T_{sw} is 125 ns.

We measured the software delay of our implementation by connecting the radio SFD pin of four Tmote Sky nodes to a logic analyzer. These four nodes act as receivers, while an additional node periodically initiates a flood. Upon overhearing a packet from the initiator, the receivers trigger a transmission, and we measure the distance between the end of a reception and the beginning of a transmission. This corresponds to $T_{sw} + T_{cal} + T_{pr} + T_f$.

Fig. 9 shows the distribution of the software delay, computed by removing the constant $T_{cal} + T_{pr} + T_f = 352\,\mu$s. We see that in 91 % of the cases the delay matches the theoretical binary distribution according to (3). Moreover, the values are equally distributed between the two possible values, 23.25 μs and 23.375 μs, for $I = 97$ in our implementation. In the remaining 9 % of the cases, an additional uncertainty of one radio clock tick affects the delay. However, this is mainly due to the drift of the DCO that may generate a frequency different from the nominal value f_p. In fact, it appears very difficult to avoid such negative drift effects, given that our implementation synchronizes the DCO with respect to the stable 32,768 Hz crystal every time Glossy starts, and the number of instructions is (at least very close to) the minimum.

5.4 Time Synchronization

Glossy provides implicit time synchronization. Receivers compute a common reference time based on the relay counter c received during the flood and the estimated slot length T_{slot}. On a Tmote Sky sensor node, the MSP430 can use two separate time sources: the internal high-frequency DCO and an external low-frequency crystal. This 32 kHz external crystal is significantly more stable than the internal DCO but provides time with low resolution. By contrast, the DCO provides sub-microsecond resolution, but does not guarantee short-term stability, and is usually disabled when the MCU enters a low-power execution mode.

We exploit the *Virtual High-resolution Time* (VHT) approach by Schmid *et al.* [27] to achieve high-resolution and low-power time synchronization. The DCO is enabled at the beginning of a Glossy phase, and the MCU does not enter a low-power mode until Glossy terminates its execution. The MCU timestamps with the high-frequency clock all the interrupts generated by transitions of the SFD pin. As a result, receivers compute high-resolution estimates of T_{slot}. The timer capture functionality of the MSP430 is then exploited to translate the high-resolution estimate of the reference time to a low-resolution value and a relative high-resolution offset. These two time values are provided to the application.

When the application schedules synchronized actions, it only needs to turn on the internal DCO and do a reverse translation to a high-resolution time value. As a result, events can be scheduled with high resolution and with an energy cost proportional to the number of timer accesses. Receivers can also exploit estimates of T_{slot} to compute the drift of the low-frequency clock. As discussed in Sec. 4.2, T_{slot} depends to a great extent on the radio clock, sourced by a high-frequency and stable crystal. Accurate synchronization between two Glossy phases can be maintained by compensating for the measured drift. We show in Sec. 7 that our synchronization implementation accurately estimates the reference time with an average error smaller than one microsecond.

5.5 Porting Glossy to Other Radios

Glossy can be ported to IEEE 802.15.4-compliant radios other than the CC2420. Destructive interference due to path delay differences is not a major problem in current low-power wireless networks, where links are rarely longer than a few tens of meters [10]. With long-range radios, the requirement for constructive interference $\Delta_{\max} = 0.5\,\mu$s corresponds to a maximum *difference* in path delay of 150 meters. However, if transmission power control is not used, such big differences in path delay would also result in big differences in received signal strength, making a correct reception of the first (stronger) packet very likely due to capture effects.

Radios like the AT86RF230 [3] feature a RAM for packet buffering. It is thus possible to change the value of certain bytes (*e.g.*, the relay counter) in-situ, that is, without the need to transfer the entire packet twice over the SPI bus between a reception and a transmission. Compared to our Tmote Sky implementation, this feature eases the effort for minimizing the software delay. Moreover, the software delay is completely eliminated in radios supporting automatic switch to transmission mode at the end of a packet reception.

6. THEORETICAL ANALYSIS

This section studies Glossy analytically. In particular, we look at the probability that Glossy makes concurrent transmissions of the same packet interfere constructively, which depends on the temporal displacement Δ among the transmissions (see Sec. 2). We want to analyze how Δ is affected by the number of concurrent transmitters (*i.e.*, node density) and the maximum hop distance of a receiver from the initiator (*i.e.*, network size). In addition, we want to study the limits of Glossy in a worst-case setting that is extremely difficult to reproduce with real sensor nodes.

To this end, we consider the network structure in Fig. 10(a). There are $m \geq 2$ *independent* flooding paths originating at the initiator. These paths traverse $h \geq 2$ hops each, and join again at a common receiver. In this way, we construct a worst-case scenario in the sense that the initiator provides the only common synchronization point to the paths: nodes on one path relay the flooding packet independently of nodes on the other paths, which challenges Glossy in making the final m concurrent transmissions interfere constructively at the common receiver.

We first present a theoretical model of the temporal displacement Δ experienced by the common receiver, independent of a specific implementation or node platform. Then, we apply this model to our implementation of Glossy on Tmote Sky devices. The results show that Glossy generates constructive interference with a probability above 99.9 % even when 30 nodes transmit concurrently.

6.1 Implementation-independent Analysis

We first analyze the sources of temporal uncertainty affecting the slot length T_{slot} given by (1). Our analysis makes use of a mixture of statistical and worst-case assumptions. We consider statistical distributions for processes that are clearly stochastic in nature, such as the offset between two unsynchronized clocks. We instead consider worst-case scenarios for more deterministic variables, including clock drift, network topology, and the maximum temporal displacement among transmitters. Hence, our model provides the statistical worst-case displacement Δ experienced by the common receiver as a function of m and h.

6.1.1 *Statistical Uncertainty on Slot Length*

We discussed in Sec. 5 that the delay T_{sw} introduced by the software routine to trigger a transmission is in general not constant, even if the number of instructions I executed by the MCU is fixed. The software delay T_{sw} is a multiple of the period $1/f_r$ of the crystal sourcing the radio clock. We can thus express the software delay as $T_{sw} = \tilde{T}_{sw} + \tau_{sw}$, where $\tilde{T}_{sw}$ is a constant value corresponding to the minimum possible delay, and τ_{sw} is a discrete random variable with granularity $1/f_r$ representing the additional variation due to the unsynchronized clocks of the MCU and the radio. We denote with p_{sw} the probability mass function (pmf) of τ_{sw}.

The processing delay of the radio, T_d, is also not constant. The digital circuits of the radio are sourced by a crystal oscillator that has frequency f_r. The radio starts to process an incoming packet when the digital circuits sampled the beginning of a reception, at most after $1/f_r$. We express the processing delay of the radio as $T_d = \tilde{T}_d + \tau_d$. The time needed to process an incoming packet, $\tilde{T}_d$, is a constant usually in the order of a few microseconds and determined by the radio. The time required to sample a reception, τ_d, depends on the offset between the radio clocks of the transmitter and the receiver. Since these clocks run unsynchronized, τ_d is a random variable with uniform distribution in the interval $[0, 1/f_r]$. We discretize the set of values of τ_d by introducing a time granularity δ such that $\delta = 1/(k \cdot f_r)$, $k \gg 1$. Consequently, τ_d has uniform discrete distribution $\tau_d = \{0, \delta, 2 \cdot \delta, \ldots, 1/f_r\}$ and pmf p_d with constant values $1/(k+1)$.

The statistical uncertainty on the length of a slot is the sum of the uncertainties on the software delay and the radio processing:

$$\tau_{slot} = \tau_{sw} + \tau_d \tag{4}$$

Since $\delta \ll 1/f_r$, τ_{slot} has granularity δ. The two uncertainties, τ_{sw} and τ_d, are independent, because they are due to independent effects. Recalling that the distribution of the sum of two independent random variables can be expressed by their convolution, the uncertainty on the length of a slot has pmf $p_{slot} = p_{sw} * p_d$.

6.1.2 *Worst-Case Drift of Radio Clock*

The time required for a packet transmission, T_{tx}, is given by (2) and depends on the frequency of the radio clock f_r. In general,

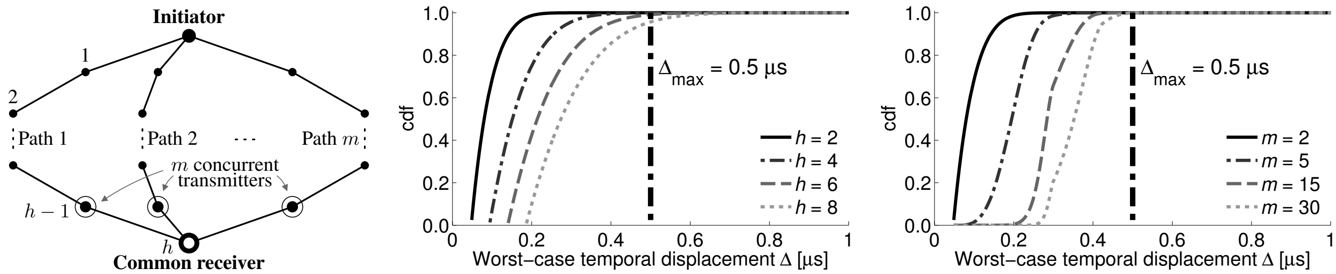

(a) Scenario: a receiver is at the end of m independent paths of length h.

(b) Distribution of Δ as a function of network size h, with $m = 2$.

(c) Distribution of Δ as a function of node density m, with $h = 2$.

Figure 10: Scenario and results of the theoretical analysis. *In our Glossy implementation, the statistical worst-case temporal displacement among all transmitters, Δ, is smaller than 0.5 μs with different network settings. Results are provided for $N = 3$.*

this frequency deviates from the nominal value $\tilde{f}_r$ due to temperature and aging effects. Crystals used to source the clocks of sensor network radios have a frequency drift ρ that depends on the temperature t according to a third-order polynomial [26]:

$$\rho = (f_r - \tilde{f}_r)/\tilde{f}_r = A(\mathrm{t} - \mathrm{t}_0)^3 + B(\mathrm{t} - \mathrm{t}_0) + C \qquad (5)$$

Here, A, B, C, and t_0 are constants that depend on the specific crystal device. Using (5), it is possible to determine bounds on the frequency drift for a given temperature range.

In the following, we assume $-\hat{\rho} \leq \rho \leq \hat{\rho}$. In the worst case, among the m independent paths in Fig. 10(a), there is at least one path where all radio clocks run at the highest frequency $\tilde{f}_r(1 + \hat{\rho})$, and at least one other path where all radio clocks run at the lowest frequency $\tilde{f}_r(1 - \hat{\rho})$. We denote with $\tilde{T}_{tx}$ the nominal transmission time in the absence of radio clock drift. With this, we can express the worst-case variation on the transmission time that accumulates after h hops at the end of these two independent paths as follows:

$$\tau_{tx} = (h - 1) \cdot \frac{2 \cdot \hat{\rho}}{1 - \hat{\rho}^2} \cdot \tilde{T}_{tx} \qquad (6)$$

6.1.3 Statistical Worst-case Temporal Displacement

Each node introduces a statistical uncertainty τ_{slot} on the length of a slot. This uncertainty is independent of other nodes, since the pair of radio and MCU clocks on one node runs independently from the pair of clocks on other nodes. Therefore, the temporal uncertainty τ associated with a path that consists of h hops is the sum of $h-1$ independent random variables $\tau = (h-1) \cdot \tau_{slot}$. The pmf of τ is given by the convolution of $h - 1$ instances of p_{slot}.

We now extend the problem to m independent paths, each consisting of h hops and originating at the initiator. We are interested in the statistical worst-case temporal displacement Δ. This displacement corresponds to the difference between the maximum and the minimum timing variation associated with each path. We consider a worst-case scenario where the path with the minimum time variation has clocks running at the highest frequency, and the path with the maximum variation has clocks running at the lowest frequency:

$$\Delta = \max_m[\tau] - \min_m[\tau] + \tau_{tx} \qquad (7)$$

Based on (7), we want to determine the cumulative distribution function (cdf) of Δ. This corresponds to the problem of finding the cdf of the sample range of m independent identically distributed (i.i.d.) experiments. This is a well-known order statistics problem, and analytical solutions exist in the literature [2].

6.2 Implementation-dependent Analysis

We now apply the above model to our Glossy implementation on Tmote Sky devices. We analyze the statistical worst-case temporal displacement Δ for different node densities and network sizes. We use the measurements shown in Fig. 9 to obtain the pmf of the software delay T_{sw}. In addition, we consider $\hat{\rho} = 20$ ppm as the maximum drift affecting the radio crystal, which corresponds to a temperature range between -30°C and 50°C [26].

To analyze the dependency on network size, we fix the number of paths at $m = 2$ and vary the path length h between 2 and 8 hops. Fig. 10(b) plots the cdf of Δ for four different settings. We see that Δ is smaller than the requirement of 0.5 μs with very high probability. This shows that when a flooding packet is relayed along two independent paths over 8 hops, the two final concurrent transmissions generate constructive interference in more than 96 % of the cases. Recall that this assumes that the time variation due to radio clock drift is maximum between the two paths. However, in reality, the drift is usually much smaller than its bounds, which increases the probability of constructive interference significantly.

To analyze the dependency on node density, we set the path length to $h = 2$ and vary the number of paths m between 2 and 30. Fig. 10(c) shows that our Glossy implementation is robust also in very dense networks. In fact, when 30 nodes transmit concurrently to a common receiver, Δ is smaller than 0.5 μs with a probability above 99.9 %. We show in Sec. 7 that experimental results from high-density networks confirm these analytical results.

6.3 Theoretical Lower Latency Bound

We provide an expression for the theoretical lower bound on flooding latency. Intuitively, this bound is given by adding up the hardware-dependent times for transmitting T_{tx} and radio processing T_d. Given that nodes transmit concurrently, the theoretical lower latency bound in a network with size h hops is $h \cdot (T_{tx} + T_d)$.

At each hop, Glossy adds a delay T_{sw} to the theoretical lower bound. This delay is introduced by the MCU when issuing a transmission request to the radio. In our implementation, T_{sw} is at most 23.5 μs (see Fig. 9). We are not aware of any flooding protocol that comes so close to the theoretical lower latency bound.

7. EXPERIMENTAL EVALUATION

This section evaluates Glossy on real sensor nodes. We first present results from experiments with a few nodes in several controlled settings. Afterwards, we report on the performance of Glossy during extensive experiments on three wireless sensor testbeds.

7.1 Glossy in Controlled Experiments

Before evaluating Glossy on several testbeds, we use controlled experiments to study some of its basic characteristics. We start by looking at the *reliability of concurrent transmissions*, defined as the fraction of packets correctly received by a node. We analyze how reliability is affected by the temporal displacement Δ between

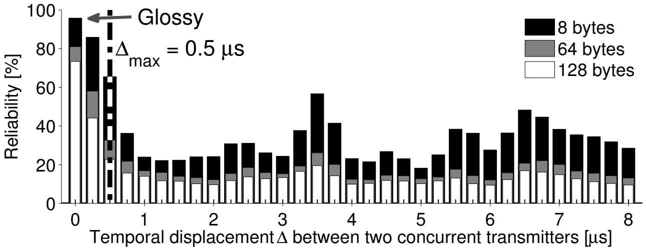

Figure 11: Glossy in a scenario without capture effects, for $N = 1$. *Reliability is 95 % due to constructive interference when the temporal displacement Δ is zero. Reliability drops significantly as Δ exceeds 0.5 μs, and follows the same pattern as in Fig. 2.*

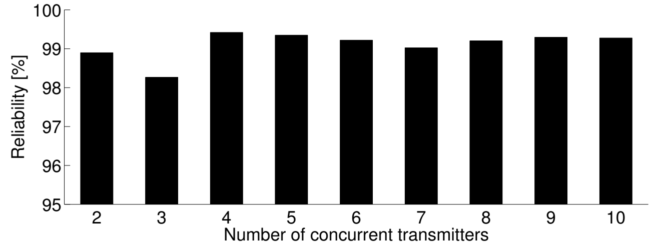

Figure 12: Reliability depending on number of concurrent transmitters, including capture effects, for $N = 1$. *Reliability is fairly constant and always above 98 %, thus showing no significant dependency on the number of concurrent transmitters.*

two transmitters and by the total number of concurrent transmitters. Afterwards, we look at the *time synchronization error*, which we define as the absolute error on the reference time computed by a receiver with respect to the initiator.

We find that (*i*) Glossy provides a reliability above 95 % *in a scenario where the capture effect does not occur*; (*ii*) while varying the number of concurrent transmitters between 2 and 10, reliability stays fairly constant and always above 98 %; (*iii*) Glossy achieves an average time synchronization error of less than 0.4 μs even at receivers that are eight hops away from the initiator.

7.1.1 Impact of Temporal Displacement

The first experiment evaluates the reliability of Glossy in a scenario where the capture effect does not occur. In this case, a successful reception is only possible if concurrent transmissions interfere constructively. While this is clearly a worst-case scenario that is difficult to reproduce even under controlled settings, it nevertheless gives an indication of Glossy's robustness.

Setup. We use three nodes, one initiator and two receivers, and set $N = 1$. Upon receiving a packet from the initiator, the two receivers transmit concurrently. The initiator overhears these transmissions and records whether it can successfully decode the packet. Based on sequence numbers embedded in the packets, we measure the reliability experienced by the initiator. Moreover, we delay the transmission of one receiver by a variable amount of time in the interval $[0, 8]\,\mu$s by letting the receiver execute a certain number of NOPs before issuing a transmission request to the radio. We set the clock frequency of the MCU to 4 MHz to obtain a temporal displacement Δ with 250 ns granularity between the two receivers, corresponding to half-chip period $T_c/2$ of the modulated signal.

To ensure that the capture effect does not help the initiator in receiving the packet, we adjust the transmit powers of the receivers. In particular, we let the non-delayed receiver transmit at -20 dBm, and the delayed receiver at -13 dBm. In this way, since both signals are weak and the second one is stronger than the first one, we prevent the initiator from capturing the first of the two signals.

Results. Fig. 11 shows reliability for different temporal displacements Δ and packet lengths, averaged over 2,000 packets for each setting. We see that the leftmost bar, corresponding to Glossy without artificial delay, indicates a reliability above 95 % for short packets. This demonstrates that Glossy makes concurrent transmissions interfere constructively, allowing a receiver to decode a packet with very high probability even in the absence of the capture effect. For increasing Δ we see a pattern similar to the one in Fig. 2 obtained through simulation. In particular, reliability starts to drop significantly at $\Delta_{\max} = 0.5\,\mu$s, showing local minima when different chips perfectly overlap. Finally, similar to non-concurrent transmissions [25], reliability decreases as packets become longer.

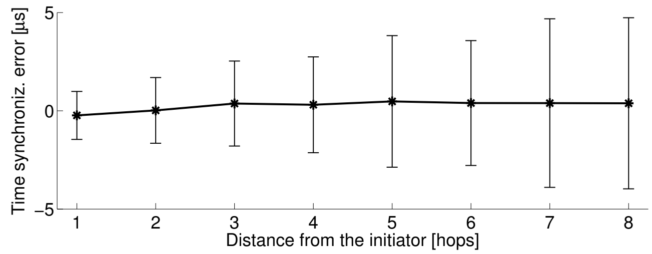

Figure 13: Accuracy of time synchronization in Glossy. *The absolute error on the reference time computed by a receiver is below 0.4 μs, even at receivers that are 8 hops apart from the initiator.*

7.1.2 Impact of Number of Concurrent Transmitters

In a typical deployment, nodes are not evenly distributed and experience different channel characteristics. As a result, some nodes have more neighbors than others. We therefore study in this experiment the impact of the number of transmitters on reliability.

Setup. We use a setup similar to the one above. However, we vary the number of receivers between 2 and 10, and do not delay their transmissions artificially; all packets are 8 bytes long. In this way, we measure the reliability experienced by the initiator for different numbers of concurrent transmitters, including capture effects.

Results. Fig. 12 shows reliability, averaged over 10,000 packets for each setting. We see that reliability stays fairly constant and always above 98 % as the number of transmitters increases, thus showing no significant dependency between the two. Interestingly, reliability is slightly lower when only two or three nodes transmit concurrently. In these settings it is more likely that the initiator receives a weak signal, due to the generation of carriers with slightly different frequencies or different phases. Our results resemble those in [11], where nodes transmit fixed-length acknowledgment packets automatically generated by the radio hardware. By contrast, Glossy transmits variable-length packets generated in software, achieving even higher reliability in some cases.

7.1.3 Accuracy of Time Synchronization

Glossy provides network-wide time synchronization at no additional cost. To this end, a receiver computes a reference time when receiving the first flooding packet, as detailed in Sec. 5.4. We assess the accuracy of this computation by looking at the absolute error with respect to the reference time computed by the initiator.

Setup. We use five nodes, one initiator and four receivers. At the beginning of a Glossy phase, the initiator sends a packet, computes a reference time, and schedules the next phase based on this reference time. The receivers do exactly the same. After receiving the packet from the initiator, they compute reference times, and use these to schedule the beginning of the next phase.

Testbed	Tx power [dBm]	Size [hops]	$N=1$ L [ms]	$N=1$ R [%]	$N=1$ T [ms]	$N=2$ L [ms]	$N=2$ R [%]	$N=2$ T [ms]	$N=3$ L [ms]	$N=3$ R [%]	$N=3$ T [ms]	$N=6$ L [ms]	$N=6$ R [%]	$N=6$ T [ms]
MoteLab (94 nodes)	0	5	1.77	99.37	3.13	1.79	99.88	4.75	1.79	99.96	6.30	1.79	> 99.99	10.87
	-7	8	2.28	94.80	4.85	2.35	99.09	5.14	2.37	99.78	6.31	2.39	99.98	10.18
Twist (92 nodes)	0	3	0.81	99.90	1.99	0.81	> 99.99	3.37	0.81	> 99.99	4.76	0.81	> 99.99	9.07
	-15	3	1.18	99.83	2.39	1.18	99.99	3.81	1.18	> 99.99	5.25	1.18	> 99.99	9.60
	-25	5	1.74	99.64	3.04	1.75	99.97	4.56	1.75	> 99.99	6.14	1.75	> 99.99	10.84
Local (39 nodes)	0	3	1.06	99.71	2.31	1.07	99.97	3.76	1.07	> 99.99	5.20	1.07	> 99.99	9.52
	-15	7	1.81	98.25	3.45	1.83	99.91	4.75	1.83	99.99	6.26	1.83	> 99.99	10.79

Table 1: Testbed configurations and results. *Tx power is the transmit power of all nodes in a testbed, and size is the corresponding maximum hop distance between initiator and receivers. We show network-wide averages of flooding latency L, flooding reliability R, and radio on-time T across four different choices of N, which is the maximum number of transmissions per node during a network flood.*

All nodes activate an external pin when a phase starts. We connect the respective pin of the five nodes to an oscilloscope, monitoring the start of a phase at a granularity of 2 ns. Then we measure the time difference between pin activation at the initiator and pin activation at the receivers. In this way, we obtain four estimates of the time synchronization error. To analyze this error for receivers that are more than one hop away from the initiator, we choose a sufficiently large N and let the receivers compute the reference time based on packets received in later slots.

Results. Fig. 13 shows average and standard deviation of the time synchronization error depending on hop distance from the initiator, averaged over 4,000 measurements for each setting. We see that the average error increases slightly up to hop 3, but then remains as low as 0.4 μs up to hop 8. The standard deviation increases almost linearly with hop distance, reaching 4.8 μs at hop 8.

These results show that Glossy achieves accurate time synchronization also at receivers that are several hops away from the initiator. Moreover, they confirm a major result of our theoretical analysis in Sec. 6, namely that Glossy accumulates only a very small timing error at each slot. Most of the error is indeed of a stochastic nature, independent across nodes and different floods.

7.2 Glossy in Testbed Experiments

Using experiments on three wireless sensor testbeds, we evaluate Glossy's performance across several node densities, network sizes, packet lengths, and transmit powers. The results demonstrate that Glossy provides robust and efficient network flooding under diverse conditions. We first describe the testbeds and metrics we use. Then we summarize our key findings, followed by a detailed discussion of the experimental results.

7.2.1 Scenario and Metrics

We use three different testbeds to evaluate Glossy: MoteLab [34], Twist [14], and a local one. These differ along several dimensions, including number of nodes, node density, and network size. On MoteLab, we collect data from 94 nodes unevenly spread over three floors. A node at the corner of the second floor acts as initiator. It reaches all other nodes within at most 5 hops when nodes transmit at the highest power setting of 0 dBm. When transmitting at -7 dBm, the lowest power that keeps the network fully connected, the farthest nodes are 8 hops away from the initiator. On Twist, we use 92 nodes and randomly choose one of them as initiator. Due to high node density, the network stays connected even at a transmit power of -25 dBm, yielding a maximum hop distance of 5 from the initiator. Our local testbed consists of 39 nodes distributed in several offices, passages, and storerooms; two nodes are located outside on the rooftop. The initiator reaches all nodes within 7 hops at the lowest possible transmit power of -15 dBm. On all three testbeds, we use channel 26 to limit the interference with co-located WiFi networks. The first section in Table 1 lists number of nodes, transmit powers, and network sizes of each testbed we use.

Our evaluation is based on the following three metrics: (*i*) *flooding latency* L of a receiver is the time between the first transmission at the initiator and the first successful reception at that receiver; (*ii*) *flooding reliability* R is the fraction of network floods in which a receiver successfully receives the packet; (*iii*) *radio on-time* T is the time a receiver has its radio turned on during a network flood. We compute these metrics for a particular setting based on 50,000 network floods. We report L, R, and T for each receiver individually as well as averaged over all receivers in a testbed.

7.2.2 Summary of Testbed Results

Table 1 summarizes the results collected on the three testbeds. It lists network-wide averages of L, R, and T across four choices of N. Our experiments reveal the following key findings:

- The empirical performance of Glossy exhibits no noticeable dependency on node density. Theoretically, performance and node density are not independent. The analysis in Sec. 6 shows that the probability of constructive interference is 99.9 % when adding 30 concurrent transmitters. However, we do not discern this marginal difference in our results from controlled experiments with up to 10 transmitters (see Sec. 7.1.2) and experiments on three testbeds, including Twist where nodes are densely deployed.
- The performance of Glossy depends on network size, that is, on the maximum hop distance between initiator and receivers. Flooding latency L and radio on-time T increase linearly, and flooding reliability R decreases logarithmically, as the network size increases. Nevertheless, for the largest size of 8 hops on MoteLab with $N = 6$, L averages around 2.4 ms, R is above 99.9 %, and T is as low as 10.2 ms.
- Increasing the maximum number of transmissions N significantly enhances flooding reliability. For $N = 3$, we observe that R is at least 99.9 % across all testbeds and transmit powers except one. Since R is already very high for $N = 1$, further increasing N has no noticeable effect on the average flooding latency. Radio on-time increases linearly with N, averaging around 16 ms for the highest value of $N = 10$ in our experiments.

In the following, we report results from Twist based on network floods with an 8-byte packet. This packet length is sufficient to send short commands to the nodes (*e.g.*, to set system parameters). We also run experiments with longer packets on MoteLab to see how the packet length affects the performance of Glossy. We find that flooding reliability decreases logarithmically as the packet length increases; for example, R is 99.26 % for $N = 3$ when nodes transmit 128-byte packets at the highest power (see Table 1). This is expected as current radios make decisions about the correctness of

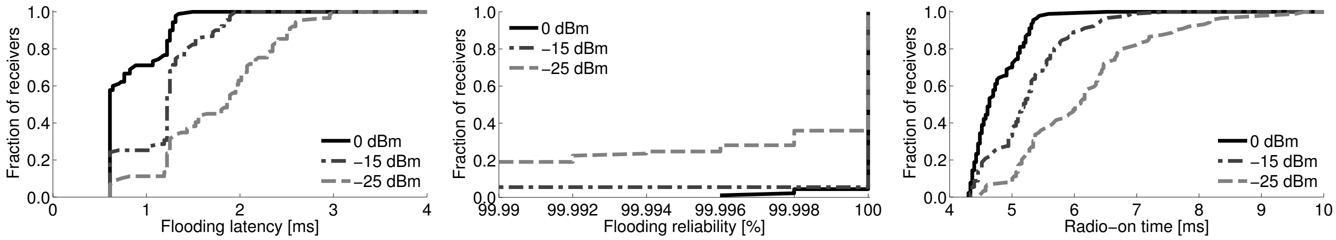

(a) Flooding latency. (b) Flooding reliability. (c) Radio on-time.

Figure 14: cdf of Glossy performance on Twist with three different transmit powers, for $N = 3$.

each individual symbol—a packet is only accepted if all symbols are correctly received. Flooding latency and radio on-time increase linearly with packet length since transmissions and receptions take longer, as described in Sec. 4.2. Overall, the results indicate that Glossy is suitable for applications that need to flood long packets.

7.2.3 Impact of Network Characteristics

We start by looking at the performance of Glossy under different network characteristics. To this end, we run experiments with three different transmit powers on Twist (see Table 1). In doing so, we effectively control the average node density in the network and the network size. We keep $N = 3$ fixed across all runs.

Fig. 14 plots the cdfs of R, L, and T for different transmit powers. We see from Fig. 14(a) that Glossy needs less than 3 ms to flood a packet to all 91 receivers, even at the lowest power that merely keeps the network connected. We are not aware of any current protocol that provides such fast flooding. We comment on related flooding and dissemination protocols in Sec. 8.

Looking at Fig. 14(b), we find that all receivers have a flooding reliability above 99.99 % at the highest power setting (*i.e.*, at the highest node density). At the lowest power, still 80 % of the receivers experience such high reliability. The drop in R is due to an increased network size. In fact, it takes 5 hops instead of 3 to reach the farthest receivers at the lowest power. This is also reflected in the step-wise shape of the cdf: each step corresponds to the flooding reliability experienced by receivers at a certain hop distance from the initiator. This observation confirms also that R exhibits no noticeable dependency on node density, as hinted by our controlled experiments in Sec. 7.1.2.

Finally, Fig. 14(c) plots the radio on-time. We see that receivers listen longer as their hop distance from the initiator increases. Nevertheless, Glossy achieves ultra-low duty cycles also for larger network sizes. For example, consider an application that wants to use Glossy to (potentially) flood a command every minute. Then, on Twist, Glossy would utilize not more than 0.01 % of a node's average radio duty cycle. We measure comparably low duty cycles on MoteLab with a maximum distance of 8 hops from the initiator.

7.2.4 Impact of Maximum Number of Transmissions

Next, we analyze how the performance is affected by N, the maximum number of transmissions per node during a network flood. We run experiments on Twist and vary N between 1 and 10. To stress Glossy as much as possible, we use the lowest possible transmit power of -25 dBm, resulting in a network size of 5 hops.

Figs. 15 and 16 plot R, L, and T for different N. Bars show network-wide averages; error bars indicate the standard deviation. Flooding reliability, shown in Fig. 15, increases almost logarithmically with N. Starting from $N = 3$, R consistently exceeds 99.99 %. In fact, we performed 50,000 floods with $N = 10$, and only in 3 cases one of the 91 receivers missed the packet.

Flooding latency, shown in Fig. 16, averages around 1.75 ms for all values of N. It is largely independent of N due to the high probability of correctly receiving a packet already at the first attempt. Given the slot length T_{slot} and the relay counter c, we can compute the flooding latency of a receiver using $L = (c+1) \cdot T_{slot}$, assuming perfect reliability.

Finally, by looking at Fig. 16, we see that the radio on-time increases linearly with N. This is also reflected in the corresponding analytical expression $T = T_w + 2N \cdot T_{slot}$, where T_w is the time a receiver listens before the first transmission it overhears. The longest radio on-time averages around 16 ms for $N = 10$.

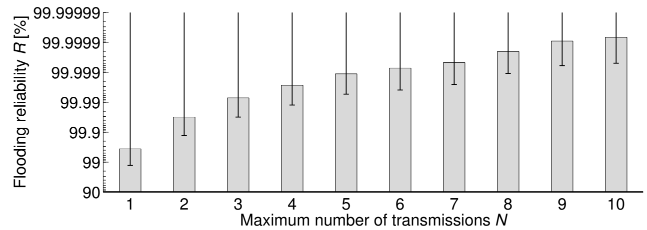

Figure 15: Flooding reliability for various N on Twist. *The average flooding reliability increases almost logarithmically with N. Within 50,000 network floods for $N = 10$, only in 3 cases one of the 91 receivers missed the packet.*

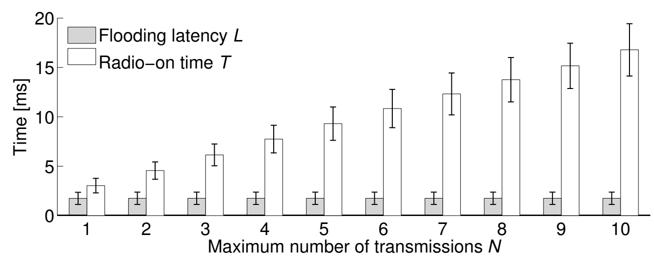

Figure 16: Flooding latency and radio on-time for various N on Twist. *Radio on-time increases linearly with N, while the average flooding latency keeps almost constant.*

8. RELATED WORK

Using Glossy, nodes transmit the same packet concurrently. This idea stems from work on cooperative communication schemes [28]. However, requirements such as precise time synchronization among multiple transmitters have long been considered too demanding for an implementation on real sensor nodes [30].

Flury and Wattenhofer demonstrate the feasibility of signaling a binary value to all nodes with an unmodulated wave [13]. Constructive interference provides the opportunity to extend this to real data packets. Dutta *et al.* propose Backcast as an acknowledged anycast service [11]. Backcast exploits constructive interference of short acknowledgment packets automatically generated by the radio hardware. It does not require synchronization among the nodes, but the application has very limited control over the content of the interfering packets. In a recent work [10], Backcast serves as the basis for A-MAC, a receiver-initiated link layer protocol. Moreover, interference has been exploited to increase the throughput of wireless networks (*e.g.*, through analog network coding [16]).

Flash [21] uses concurrent transmissions for rapid flooding in sensor networks. Flash relies exclusively on capture effects, which considerably reduces the chances of correct packet reception when many nodes transmit concurrently [21]. Glossy also benefits from capture effects but primarily exploits constructive interference. This enables Glossy to flood packets with high reliability at any node density, as demonstrated by our testbed experiments in Sec. 7.2.

Glossy and Flash do not require nodes to maintain information about the network topology. By contrast, in the Robust Broadcast Protocol (RBP) [29] and the Collective Flooding (CF) [38] nodes need to continuously collect information about their local neighborhood to identify links important for the broadcast propagation.

Trickle [19] and its variants provide data dissemination: nodes continuously send advertisements to detect new data and ensure complete network coverage. Typically, dissemination protocols are optimized for reliability and data consistency, not for latency or energy. Glossy floods packets fast without additional control traffic, while sacrificing less than 0.01 % in flooding reliability.

Flooding is a basic communication primitive for time synchronization in sensor networks. For example, the Flooding Time Synchronization Protocol (FTSP) [22] uses periodic flooding of time-stamped messages and achieves a per-hop synchronization error in the microsecond range. Lenzen *et al.* show that optimal synchronization necessitates fast network flooding [18]. Their PulseSync protocol achieves a higher accuracy than FTSP and a flooding latency below one second. Glossy provides even higher accuracy by flooding packets within a few milliseconds and employing the Virtual High-resolution Time (VHT) approach by Schmid *et al.* [27]. The high accuracy and low energy of VHT are also due to the use of a custom external high-speed crystal [27]. Glossy could enable further improvements in synchronization accuracy by combining it with such crystals.

9. CONCLUSIONS

This paper is motivated by real-world sensor network systems that rely on fast network flooding and accurate time synchronization. We observe that such systems would significantly benefit from a service that integrates both functionalities in an efficient manner. This paper thus proposes Glossy, a novel flooding architecture for wireless sensor networks that uses interference to its advantage. By making simultaneous transmissions of the same packet interfere constructively, Glossy enables receivers to decode a packet even in the absence of capture effects. We have analyzed the robustness of our techniques in achieving constructive interference based on a mixture of stochastic and worst-case models. We have evaluated our implementation of Glossy using experiments under controlled settings and on three wireless sensor testbeds. The results demonstrate that Glossy provides accurate time synchronization along with fast and highly reliable flooding at ultra-low duty cycles, showing no noticeable dependency on node density in the scenarios considered. The source code of Glossy is publicly available at `http://www.tik.ee.ethz.ch/~ferrarif/sw/glossy`.

Acknowledgments. The authors thank Matthias Keller, Luca Mottola, and Thiemo Voigt for their feedback on early versions of this paper, and the anonymous reviewers for their helpful comments. This work was supported by Nano-Tera and the National Competence Center in Research on Mobile Information and Communication Systems (NCCR-MICS), a center supported by the Swiss National Science Foundation under grant number 5005-67322.

10. REFERENCES

[1] The Contiki operating system. `http://www.sics.se/contiki/`.
[2] B. C. Arnold, N. Balakrishnan, and H. N. Nagaraja. *A First Course in Order Statistics*. SIAM, 2008.
[3] Atmel. AT86RF230 datasheet, 2009.
[4] G. Barrenetxea, F. Ingelrest, G. Schaefer, M. Vetterli, O. Couach, and M. Parlange. SensorScope: Out-of-the-box environmental monitoring. In *ACM/IEEE IPSN*, 2008.
[5] J. Choi, M. Kazandjieva, M. Jain, and P. Levis. The case for a network protocol isolation layer. In *ACM SenSys*, 2009.
[6] J. Chuang. The effects of time delay spread on portable radio communications channels with digital modulation. *IEEE J. Sel. Areas Commun.*, 5(5), 1987.
[7] D. Davis and S. Gronemeyer. Performance of slotted ALOHA random access with delay capture and randomized time of arrival. *IEEE Trans. Commun.*, 28(5), 1980.
[8] A. Dutta, D. Saha, D. Grunwald, and D. Sicker. SMACK – a SMart ACKnowledgment scheme for broadcast messages in wireless networks. In *ACM SIGCOMM*, 2009.
[9] P. Dutta and D. Culler. Practical asynchronous neighbor discovery and rendezvous for mobile sensing applications. In *ACM SenSys*, 2008.
[10] P. Dutta, S. Dawson-Haggerty, Y. Chen, C. M. Liang, and A. Terzis. Design and evaluation of a versatile and efficient receiver-initiated link layer for low-power wireless. In *ACM SenSys*, 2010.
[11] P. Dutta, R. Musăloiu-E., I. Stoica, and A. Terzis. Wireless ACK collisions not considered harmful. In *ACM HotNets*, 2008.
[12] A. Ephremides and T. Truong. Scheduling broadcasts in multihop radio networks. *IEEE Trans. Commun.*, 38(4), 1990.
[13] R. Flury and R. Wattenhofer. Slotted programming for sensor networks. In *ACM/IEEE IPSN*, 2010.
[14] V. Handziski, A. Köpke, A. Willig, and A. Wolisz. TWIST: A scalable and reconfigurable testbed for wireless indoor experiments with sensor networks. In *ACM REALMAN*, 2006.
[15] IEEE. std. 802.15.4-2003, 2003.
[16] S. Katti, S. Gollakota, and D. Katabi. Embracing wireless interference: analog network coding. In *ACM SIGCOMM*, 2007.
[17] K. Leentvaar and J. Flint. The capture effect in FM receivers. *IEEE Trans. Commun.*, 24(5), 1976.
[18] C. Lenzen, P. Sommer, and R. Wattenhofer. Optimal clock synchronization in networks. In *ACM SenSys*, 2009.
[19] P. Levis, N. Patel, D. Culler, and S. Shenker. Trickle: A self-regulating algorithm for code propagation and maintenance in wireless sensor networks. In *USENIX NSDI*, 2004.
[20] D. Li, K. Wong, Y. Hu, and A. Sayeed. Detection, classification, and tracking of targets. *IEEE Signal Process. Mag.*, 19(2), 2002.
[21] J. Lu and K. Whitehouse. Flash flooding: Exploiting the capture effect for rapid flooding in wireless sensor networks. In *IEEE INFOCOM*, 2009.
[22] M. Maróti, B. Kusy, G. Simon, and A. Lédeczi. The flooding time synchronization protocol. In *ACM SenSys*, 2004.
[23] S. Ni, Y. Tseng, Y. Chen, and J. Sheu. The broadcast storm problem in a mobile ad hoc network. In *ACM/IEEE MobiCom*, 1999.
[24] M. Rossi et al. SYNAPSE: A network reprogramming protocol for wireless sensor networks using fountain codes. In *IEEE SECON*, 2008.
[25] Y. Sankarasubramaniam, I. Akyildiz, and S. McLaughlin. Energy efficiency based packet size optimization in wireless sensor networks. In *SNPA*, 2003.
[26] T. Schmid. *Time in Wireless Embedded Systems*. PhD thesis, UCLA, 2009.
[27] T. Schmid, P. Dutta, and M. Srivastava. High-resolution, low-power time synchronization an oxymoron no more. In *ACM/IEEE IPSN*, 2010.
[28] B. Sirkeci-Mergen, A. Scaglione, and G. Mergen. Asymptotic analysis of multistage cooperative broadcast in wireless networks. *IEEE Trans. Inf. Theory*, 52(6), 2006.
[29] F. Stann, J. Heidemann, R. Shroff, and M. Murtaza. RBP: Robust broadcast propagation in wireless networks. In *ACM SenSys*, 2006.
[30] A. Swami, Q. Zhao, and Y. Hong. *Wireless Sensor Networks: Signal Processing and Communications*. Wiley, 2007.
[31] Texas Instruments. CC2420 datasheet, 2007.
[32] Texas Instruments. MSP430F1611 datasheet, 2009.
[33] G. Werner-Allen, K. Lorincz, J. Johnson, J. Lees, and M. Welsh. Fidelity and yield in a volcano monitoring sensor network. In *USENIX OSDI*, 2006.
[34] G. Werner-Allen, P. Swieskowski, and M. Welsh. MoteLab: A wireless sensor network testbed. In *ACM/IEEE IPSN*, 2005.
[35] B. Williams and T. Camp. Comparison of broadcasting techniques for mobile ad hoc networks. In *ACM MobiHoc*, 2002.
[36] S. Yoshida and F. Ikegami. A comparison of multipath distortion characteristics among digital modulation techniques. *IEEE Trans. Veh. Technol.*, 34(3), 1985.
[37] J. Zhao and R. Govindan. Understanding packet delivery performance in dense wireless sensor networks. In *ACM SenSys*, 2003.
[38] T. Zhu, Z. Zhong, T. He, and Z.-L. Zhang. Exploring link correlation for efficient flooding in wireless sensor networks. In *USENIX NSDI*, 2010.